

Distribution Agreement

In presenting this thesis as a partial fulfillment of the requirements for a degree from Emory University, I hereby grant to Emory University and its agents the non-exclusive license to archive, make accessible, and display my thesis in whole or in part in all forms of media, now or hereafter known, including display on the world wide web. I understand that I may select some access restrictions as part of the online submission of this thesis. I retain all ownership rights to the copyright of the thesis. I also retain the right to use in future works (such as articles or books) all or part of this thesis.

Jonathan Zawadzki

Date: 11 April 2017

Mechanism of Tetrameric Transmembrane Influenza A/M2 Proton Channel Activation

By

Jonathan Zawadzki

R. Brian Dyer

Adviser

Department of Chemistry

R. Brian Dyer

Adviser

Emily Weinert

Committee Member

Sonal Nalkur

Committee Member

2017

Mechanism of Tetrameric Transmembrane Influenza A/M2 Proton Channel Activation

By

Jonathan Zawadzki

R. Brian Dyer, PhD

Adviser

An abstract of

A thesis submitted to the Faculty of Emory College of Arts and Sciences

of Emory University in partial fulfillment

of the requirements of the degree of

Bachelor of Arts with Honors

Department of Chemistry

2017

Abstract

Mechanism of Tetrameric Transmembrane Influenza A/M2 Proton Channel Activation

By Jonathan Zawadzki

Influenza is a common infection caused by the influenza virus, presentation of which can vary from the fever and headache of the contemporary Avian flu to the fatal Spanish flu pandemic of 1918. Replication of this virus is dependent on increased proton conductance through an activated viral transmembrane M2 proton channel, a 96-residue homotetramer. In order to develop methods to control influenza replication, the proton channel's structure and function have been intensively studied. The primary objective of this study was to observe clear evidence for proton channel conformational change in which the C-termini dilates when exposed to low biologic pH (pH 4.5-6). This was accomplished using Forster Resonance Energy Transfer (FRET) analysis on donor and acceptor fluorophore labeled C-termini to determine dilation change. With a pH drop from 6.0 to 4.5, the C-termini were found to dilate from 3.0 to 3.4 nm in length, presumably allowing increased proton transport. Understanding the mechanism by which the structure of M2 proton channel activates in lower pH ranges may help develop new treatments for influenza infections.

Mechanism of Tetrameric Transmembrane Influenza A/M2 Proton Channel Activation

By

Jonathan Zawadzki

R. Brian Dyer, PhD

Adviser

An abstract of

A thesis submitted to the Faculty of Emory College of Arts and Sciences

of Emory University in partial fulfillment

of the requirements of the degree of

Bachelor of Arts with Honors

Department of Chemistry

2017

Table of Contents

I.	Introduction	1
	M2 Proton Channel and Influenza A Virus.....	1
	Structure and Function of M2 Transmembrane Domain.....	2
	FRET: Forster Resonance Energy Transfer.....	4
	M2 Proton Channel Conformation Change Measured by FRET.....	5
	Purpose	7
II.	Experimental	7
	Peptide Synthesis and Cleavage	7
	Optimal FRET Pair	8
	Labeling Peptide with Dye Molecules.....	9
	Mass Spec on Finished Labeled Peptide.....	10
	M2 Recombination to Membrane	11
	Fluorescence Measurement.....	12
III.	Results and Discussion	12
	Absorbance of Free Dye in Different pH Environments.....	12
	Tetramerization and pH Dependence of M2 Proton Channel.....	13
	Control experiment: N-termini labeled M2.....	16
	FRET Efficiency and Distance.....	17
IV.	Discussion and Improvements to the Experimental Procedures	24

List of Figures

Figure 1. Influenza virus life Cycle. The M2 proton channels function as the virion is contained in the endosome to allow uncoating (Pinto).....	1
Figure 2. M2 proton channel and its hydrophobic pore lining residues. Histidine Residues act as a filter, allowing exclusively proton while tryphophan acts as an activation gate (Acharya)..	1
Figure 3. A) M2 proton channel inhibited by amantadine (Gleed) B) Amantadine Structure.	3
Figure 4 M2 proton channel conformational change due to increase in acidity. Histidine residues repel each other (Acharya).....	3
Figure 5. The energy of the donor transfers to the acceptor as it quenches and/or fluoresces (Lakowicz).....	4
Figure 6. Combinations of homotetramer labeling ratios formed from donor and acceptor monomers.....	6
Figure 7. DABCYL and EDANS chemical structure.....	9
Figure 8 Cysteine-maleimide reaction for labeling peptides.	10
Figure 9. EDANS fluorescence and DABCYL Plus in varying pH. a) DABCYL Plus absorbance was measured as the DABCYL Plus was added to separate citrate phosphate buffers of pH 5, 5.5, 6, 6.5, 7, 7.5, and 9.2. b) EDANS fluorescence was found in the same way.	13
Figure 10. Fluorescence change as amantadine and detergent twin 20 are added to M2 reconstituted in bicelle DPPC/DHPC. When amantadine was added, the fluorescence dropped.	14
Figure 11. Fluorescence change as the acidity of the M2 tetramers were reconstituted in bicelle DPPC/DHPC. As the acidity increases, the fluorescence increases as well.....	15
Figure 12. N-termini FRET Experiment A) 1:1 DABCYL Plus to EDANS C-termini dyed peptide. Fluorescence intensity of EDANS decreases as pH increases. B)1:1 DABCYL Plus to EDANS N-termini dyed peptide. EDANS fluorescence is unchanged with change of pH.	17
Figure 13. FRET efficiency of M2 responding to pH. Varying (r) ratios differ the population of each species and therefore changes the FRET efficiency corrected by concentration.....	20
Figure 14. Different D/A ratios at pH 7.33. The Experimental data is overlaid on the theoretical results. Probability of each tetramer species forming also is shown.....	21
Figure 15. A) pH vs. FRET efficiency curve of (r) =0.125, fit to Henderson-Hasselbalch curve. pKa of 5.1 ± 0.3 while the drug bound state had a pKa of 5.1 ± 0.2 . B) pH vs. FRET efficiency curve of r=2. Fitted to Henderson-Hasselbalch curve. pKa of 5.2 ± 0.3 while its drug bound state had a pKa of 5.2 ± 0.2	22
Figure 16. . Averaged distance of all the (r) values dependent on pH. Range of 3.0-3.4 nm.B)1:1 DABCYL Plus to EDANS N-termini dyed peptide. EDANS fluorescence is unchanged with change of pH.	23
Figure 17. Alexa Fluor 546 chemical structure.....	25

List of Tables

Table 1. Distance between Leu46s of diagonal monomers in different M2 structures from Protein Data Bank.9

Table 2. The FRET efficiencies of the possible pathways between donor and acceptor pairs.....18

Table 3. The probability and FRET efficiency of each tagged M2 species in terms of (r) ratio.19

Introduction

The M2 Proton Channel and Influenza Virus

The influenza virus is ubiquitous and can be fatal. A century ago, the Spanish flu pandemic of 1918 killed 50 million people. Even today, half a million people succumb to influenza each year.¹

Replication of the virus occurs as follows: A eukaryotic target cell, as a form of defense, endocytoses an influenza virion. Upon entering the acidic environment of the late endosome (pH 5-6), the virion's M2 proton channel conducts excess protons from the endosome to the viral interior. Protons conducted through this channel acidify the virus interior, a step necessary for the eventual release of viral RNA.² The acidification of the interior provides the proper mechanism for the influenza virion to release its RNA content as the cell produces more influenza virus (Figure 1). Blocking this channel limits viral replication.² Four FDA approved drugs have been developed. Of those four, two target the viral M2 proton channel.

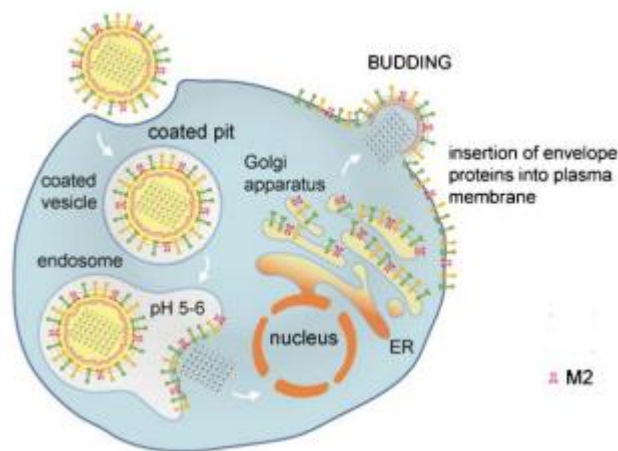


Figure 1. Influenza virus life cycle. The M2 proton channels function as the virion is contained in the endosome to allow uncoating (Pinto).²

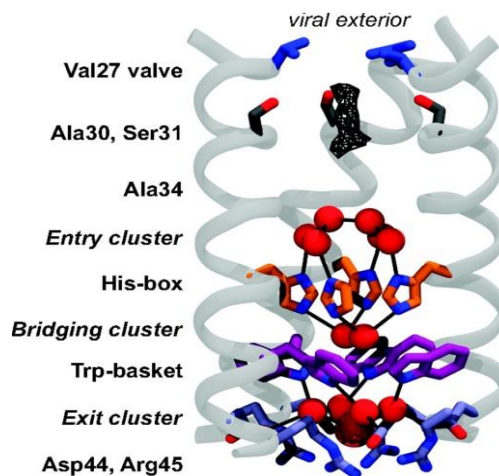


Figure 2. M2 proton channel and its hydrophobic pore lining residues. Histidine Residues act as a filter, allowing exclusively proton while tryptophan acts as an activation gate (Acharya).³

Structure and Function of the M2 Proton Channel Transmembrane Domain

The M2 proton channel transmembrane domain consists of four alpha helix monomers, each composed of 96 mostly hydrophobic amino acid residues³. This forms a homotetrameric channel pore with hydrophobic pore-lining amino acid residues. The valine residues from each monomer form the neck of this channel (Figure 2). These Val27 residues form a ring of methyl groups that constricts the N-terminal side of the pore to $\sim 3.1 \text{ \AA}$, preventing water molecules from penetrating the channel.⁴

Another vital residue within the M2 proton channel pore is histidine, which acts as a filter to conduct protons at a very high selectivity (Figure 2).³ The four His37 residues contain imidazole groups which conduct the protons through a shuttling mechanism, in which the imidazole is protonated and then deprotonated.⁴

Tryptophan residues, a few amino acids away from these histidines, ensure that histidine shuttling is unidirectional. The Trp41 residues act as a gate in response to pH. When the pH is below a certain threshold, protons are conducted into the viral interior. If the pH increases above a threshold, Trp41 residues will block proton conduction. This system ensures that the transfer of protons is unidirectional, as mutagenesis experiments replacing Trp41 with alanine, cysteine, or phenylalanine found bidirectional conductance. Histidine residues are the selective filter while tryptophan residues act as a gate ensuring unidirectionality.⁴ This unidirectionality trait conducts protons from the N-termini end (near Val27) to the C-termini (near Trp41).

Amantadine and its derivative rimantadine are anti-viral drugs that prevent the M2 proton channel's inward conduction of protons. Amantadine, the prototypic M2 proton channel inhibitor, consists of an adamantane backbone with an amino group substituted at one of the four methyne positions. Adamantane interacts with various hydrophobic residues by the channel's N-

termini, and the amino group forms hydrogen bonds with the imidazole residues of the His37s. Previous studies demonstrate amantadine's fitting within the proton channel and blocking proton conduction (Figure 3).³ Through NMR and X-ray crystal structures, it has been shown that amantadine constricts the pore and C-termini dilation.²

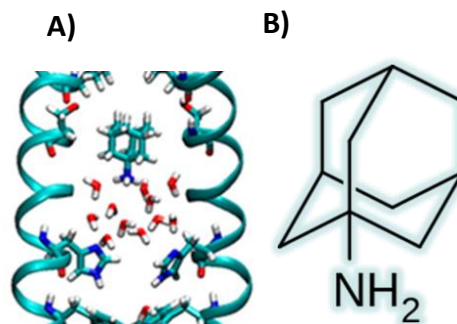


Figure 3. A) M2 proton channel inhibited by amantadine (Gleed).⁸ B) Amantadine.

Lower pH causes the M2 proton channel's C-termini to dilate, activating its proton conductance. Upon entry into the acidic environment of the endosome, each His37 residue is further protonated. The greater the excess positive charge of each His37 residue, the further they repel each other, causing a dilation of the C-termini (Figure 4).³ This conformational change is known as the M2 proton channel's activation mechanism, in which it begins to conduct protons. From previous studies, it is generally understood, but occasionally disputed, that the M2 proton channel's N-termini are fairly static whereas the C-termini are very flexible and often dilated.³ However, no experiment has confirmed the dilation in response to pH. The C-termini dilation is merely a pattern displayed by some NMR and X-ray crystal structures, although these modalities may change M2 conformation. In addition, NMR and X-ray crystal structural analyses have not controlled for environment while examining the effects of acidity on the distances between the C-termini. As a result, many researchers disagree on the activation mechanism of C-termini fluctuation.³

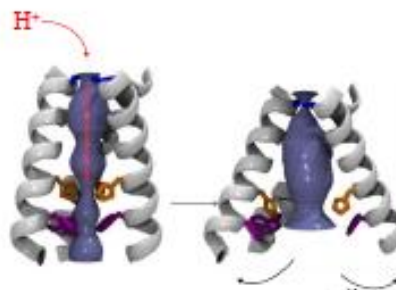


Figure 4. M2 proton channel conformational change due to increase in acidity. Histidine residues repel each other (Acharya).³

FRET: Forster Resonance Energy Transfer

Forster Resonance Energy Transfer (FRET) is a biological technique used to measure lengths on nanometer scale, and frequently used in protein structure analysis. FRET is used as a sensitive molecular ruler in biology and is a useful technique in measuring conformational changes of proteins. Donor and acceptor fluorophores are added to separate segments of a protein. An acceptor quenches donor fluorescence and may fluoresce itself. The difference in fluorescence intensity of the donor or acceptor will indicate the distance between the two fluorophores.⁵

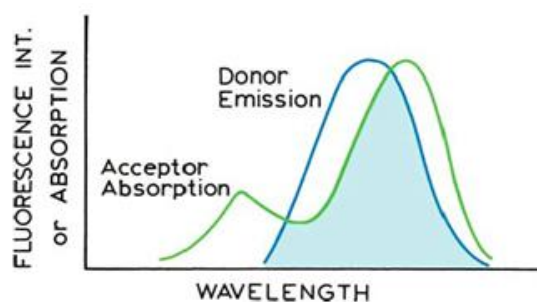


Figure 5. Spectra Overlap of donor fluorescence and acceptor absorption. The energy of the donor transfers to the acceptor as it quenches and/or fluoresces (Lakowicz).⁵

Fluorescence is the measurement in which a fluorophore, or fluorescent molecule, absorbs incident radiation that brings an electron to a higher energy state. This higher state only lasts briefly (usually in the pico- or nano-second scale) before the electron returns to its ground state while releasing energy primarily in the form of light. The light emitted by a fluorophore will have lower energy and therefore will have an increased wavelength.⁵

FRET is the measurement of a non-radiative energy transfer between a donor and an acceptor molecule, which is highly dependent on the distance between them. Irradiation corresponding to the absorbance of the donor molecule is emitted, exciting the donor. Yet, upon the electron's returning to the ground state, rather than releasing light energy, it nonradiatively excites the acceptor molecule, and in turn the acceptor molecule emits its own specific light of a certain wavelength or simply quenches the donor fluorescence.⁵

FRET efficiency (E) is the fraction of energy transfer between donor and acceptor. FRET efficiency is the difference in donor fluorescence with a nearby acceptor as compared to the donor fluorescence out of range of the acceptor. FRET efficiency is calculated by $E = 1 - F'_D/F_D$, where F'_D is the donor fluorescence intensity nearby the acceptor, and F_D is the donor fluorescence intensity out of range of the acceptor.

FRET efficiency can also be obtained from fluorescence lifetime, defined as $E = 1 - \tau'_D/\tau_D$, which is the time a fluorophore spends in the excited state before returning to the ground state. The lifetime of a fluorophore is specifically the time that must elapse for 36.7% of the population of fluorophores to return to ground state after excitement. The population of excited fluorophores is $N(t) = N_0 * e^{-t/\tau}$, where N_0 is the initial the population of excited donor fluorophore, t is the amount of time that has taken place since excitation and τ is the lifetime.⁵ The nearer the donor and acceptor fluorophores are to each other, the shorter the amount of time the donor will remain in the excited state. Lifetime fluorescence measurement is often more accurate because, unlike fluorescence intensity, it is not concentration dependent.

From FRET efficiency measurements, length can be calculated by, $E = \frac{1}{1 + (\frac{r}{R_0})^6}$, where R_0 is the Forster radius, and r is the distance between the donor and acceptor. The Forster Radius is the distance in which the FRET efficiency is 50%. FRET efficiency depends on the specific pair of donor and acceptor fluorophores, termed a FRET pair. Therefore, a protein, depending on the length of its conformation, has specific FRET pairs best suited for measuring its motion.

M2 Proton Conformation Change Measured by FRET

To measure the dilation of the channel, either a donor or acceptor fluorophore was added to the C-terminus of each M2 monomer. As the M2 proton channel is activated, the distance

between the C-termini should increase, and therefore the energy transfer between fluorophores should

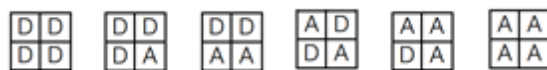


Figure 6. Possible combinations of homotetramer labeling ratios formed from donor and acceptor monomers⁷.

decrease as well. There is, however, additional

complexity. When each C-terminus of the tetramer is tagged, there are four fluorophores attached. As a result, each M2 proton channel will have various combinations of donors and acceptors that interact to impact overall fluorescence intensity (Figure 6).

Tetramer assembly will bring multiple fluorophores within the distance of fluorophore interaction. As a proton channel tetramerizes, there are six potential combinations of donor/acceptor dye molecules (Figure 6).⁷ Yet one particular combination consisting of four acceptor molecules will not fluoresce as the specific acceptor molecules in the experiment are exclusively quenchers. As a result, five remaining possible donor/acceptor molecule combinations will contribute to the FRET population with a measurable signal, i.e. the FRET efficiency. Each combination has a fluorescence contribution, which yields the approximate length of the C-termini dilation. Three assumptions must be made: 1) Both the acceptor and the donor tagged monomers coassemble randomly into possible tetramer conformations. 2) The acceptor and donor tagged monomers exist only in tetrameric form. 3) All channels are simplified as being fourfold symmetric.⁷

Although the M2 proton channel is most likely not a perfect square, as indicated by NMR and X-ray crystal structures, it can be approximated as such (Table 2). Therefore, two adjacent monomers are assumed have a distance of R , while two diagonal monomers have distance of $\sqrt{2}R$.

Purpose

Previous research has proposed that the M2 proton channel's C-termini dilate as an activation mechanism in response to increased acidity in an endosome. Crystallization required for NMR or X-ray structure study can result in artefactual conformational change, thereby undermining structural assumptions. In addition, the channel has been studied with varying compositions of lipid membrane, peptide lengths, temperatures, and other experimental conditions, but pH-related change has not been studied. This project is to determine if low pH relates to C-termini dilation under biologically relevant conditions. FRET allows us to measure conformational changes at room temperature and without the need for crystallization. Overall, better understanding the M2 proton channel's low pH activation mechanism will pave way for the next generation of effective drugs.

Experimental

Peptide Synthesis and Cleavage

To create the proper peptide monomer, Solid-Phase Peptide Synthesis (SPPS) was performed with a Liberty Blue-Automated Microwave Peptide Synthesizer. An extra cysteine amino acid was added for fluorescent tagging. The final peptide sequence was: SSDPLVVAASIIGILHLILWILDRLC for C-terminus labeled peptide and CSSDPLVVAASIIGILHLILWILDRL for N-terminus labeled peptide as a control. As previously described, the C-termini have been reported to be much more conformationally flexible than the N-termini. The purpose of N-terminus tagged peptides were to serve as control in order to attribute FRET changes solely on C-termini dilation changes and not to other factors described in the Results section below.

After synthesis, peptides attached to resin were cleaved and de-protected when exposed to a peptide cleavage solution comprised of 90% Trifluoroacetic acid (TFA), 5% thioanisole, 3% 1,2-ethanedithiol, and 2% anisole for two hours. The resin was filtered, and the resulting filtrate was added to cold ether to precipitate peptide. The precipitate and filtrate was centrifuged three times to isolate the peptide from the ether. The peptide was then dried in a desiccator and purified through means of High Powered Liquid Chromatography (HPLC). To purify the peptides, an RP-HPLC C3 column was used with a linear gradient of two buffers: Buffer B (6:3:1 isopropanol, acetonitrile, and water containing .1% TFA) vs. Buffer A (Water containing .1% TFA). The purified product was confirmed as M2 proton channel by Matrix Assisted Laser Desorption/Ionization (MALDI).

Optimal FRET Pair

The distance between the C-termini of the M2 proton channel was previously found by analyzing crystal structures under varying pH and measuring the range of the C-termini distances found in the Protein Data Bank website (<http://www.rcsb.org/pdb/home/home.do> verified April 2017). The diagonal distance between the C-termini leucine residues (measured from alpha carbon to alpha carbon) was measured. The average of all these structures at basic pH (6.5-8.8) was 2.63 nm, while the lone structure at acidic pH (5.3) showed a distance of 3.454 nm (Table 1). The FRET pair must be hydrophilic and pH independent. If the fluorophores were to be hydrophobic, it may fold back into the membrane, possibly preventing tetramer formation. In addition, the fluorophores must be pH-independent to give us an accurate distance measurement of C-termini dilation with regards to pH change. As discussed, FRET efficiency is sensitive to changes in distances around the Forster Radius. Therefore, a FRET pair with a Forster radius of

around 3 nm will be most effective. The FRET pair, (5-((2-Aminoethyl)amino)naphthalene-1-sulfonic acid) (EDANS) and 4-((4-(dimethylamino)phenyl)azo)benzoic Acid, Succinimidyl Ester (DABCYL Plus) were chosen. These fluorophores are hydrophilic, pH independent, and have a Forster radius of 3.3 nm.

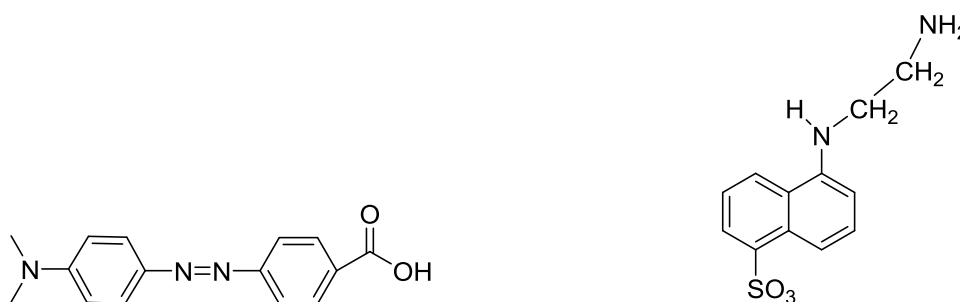


Figure 7. DABCYL (DABCYL Plus structure not available)

EDANS

Table 1. Distance between diagonal Leu46s of monomers in M2 structures from Protein Data Bank

	pH	D1 (nm)	D 2 (nm)	Condition
3BKD	5.3	3.595	3.313	X-ray, octyl- β -d-glucopyranoside detergent, With Amantadine
3LBW	6.5	2.336	2.299	X-ray, n-octylglucoside detergent
1NYJ	7	2.842	2.846	SS-NMR, DMPC lipid(C14)
2RLF	7.5	2.407	2.396	S-NMR, DHPC detergent(C4), With Rimantadine
2KAD	7.5	2.97	2.97	SS-NMR, DLPC lipid(C12), With Amantadine
2KQT	7.5	2.416	2.416	SS-NMR, DMPC lipid, With Amantadine
2LOJ	7.5	2.93	2.88	SS-NMR, DOPC/DOPE bilayer
2H95	8.8	2.572	2.572	SS-NMR, DMPC bilayer,

Labeling Peptides with Fluorophores

After an established FRET pair was chosen, the synthesized and cleaved peptides were tagged with either EDANS or DABCYL Plus. This was accomplished through a cysteine-maleimide reaction. Five milligrams of M2 peptide were placed in a 2 ml solution of 60% tetrafluoroethylene, 20% water, and 20% pH 7 phosphate buffer. The solution was titrated to pH 6-8 with 10 mM of NaOH to optimize the cysteine-maleimide reaction. To tag peptides,

approximately 0.3 mg of either maleimide EDANS or DABCYL Plus fluorophore dye were added to the solution. The peptides were tagged with the fluorophore dyes separately by incubating at room temperature for an hour.

The cysteine residue previously added to the C-terminus reacted with the maleimide attached to the fluorophore (Figure 8). After completion of the cysteine-maleimide reaction, the peptide with the fluorophore attached was purified by means of HPLC.

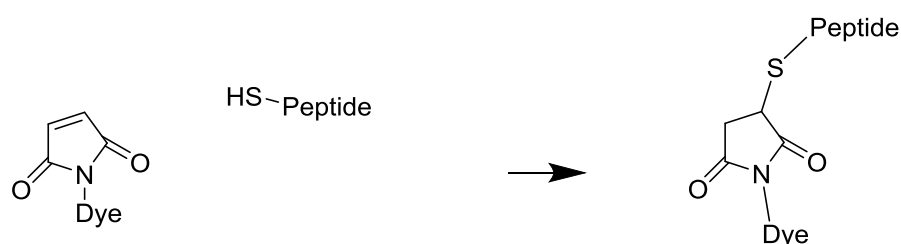


Figure 8. Cysteine-maleimide reaction. Peptide monomer is tagged with fluorophore dye.

Mass Spectrometry on Finished Labeled Peptide

After purification, to ensure the fluorophore was successfully added to the peptide monomer, the mass was determined. M2 monomers without fluorophore weigh 2831 g/mol. With a fluorophore added, the mass increases by the molecular weight of that fluorophore and the maleimide. MALDI is a soft ionization technique used to measure the mass of a biomolecule or large polymer. The molecule, in this case M2 with maleimide and fluorophore, is added to an ion source matrix α -Cyano-4-hydroxycinnamic acid (CHCA). Matrix was prepared by 0.75 ml of DI water and 0.75 ml of acetonitrile added with 0.015 g of CHCA. Using laser energy, the peptides were ionized. A mass to charge ratio was determined to confirm the fluorophore was successfully added. However, MALDI proved to be particularly difficult due to interference since the MALDI laser emits at 355 nm, and EDANS fluorophore absorbance maxima occurs at

335 nm. As a result, low signal and fragmented peaks were found. It was often quite difficult to test whether the cysteine-maleimide reaction had completed.

To alleviate this problem, Electrospray Ionization (ESI) was used instead of MALDI. Using ESI and an electromagnetic field rather than a laser to ionize the peptide, there was less fragmentation, and clear product peaks.

M2 Tetramer Formation by Reconstitution to Membrane

Fluorophore tagged monomers were reconstituted to tetramers in lipid bilayers composed of Dipalmitoylphosphatidylcholine (DPPC) and 1,2-Diheptanoyl-sn-Glycero-3-Phosphocholine (DHPC) bicelles. Buffers of varying acidities contained 100 mM solute (either phosphate, citrate, or tris depending on pH) and 100 mM NaCl. Both EDANS and DABYCL Plus labeled monomers were dissolved into ethanol, and concentrations measured by spectrophotometric absorbance of fluorophore. Beer's law calculations included EDANS extinction coefficient of $5900 \text{ L mol}^{-1} \text{ cm}^{-1}$ (335 nm) and DABCYL Plus extinction coefficient of $32,000 \text{ L mol}^{-1} \text{ cm}^{-1}$ (453 nm).⁵ Labeled M2 monomer aliquots were dried with inert nitrogen gas. Bicelles were created by hydrating and sonicating previously prepared dried lipid cake of DHPC and DPPC. The bicelle solution and M2 monomer solution were mixed, sonicated, and underwent several cooling and thawing cycles under liquid nitrogen. Tetramers were then reconstituted from monomers. We achieved a lipid to M2 tetramer ratio of 50:1. Each sample consisted of 10 μM of M2 tetramer in a bilayer consisting of 50 mM of DHPC and 10 mM of DPPC. M2 tetramers reconstituted in bicelles were exposed to 4 ml of phosphate, citrate, or tris buffers varying between pH 4 to 9. 100 μM of amantadine was then added for a second test variable.

Florescence Measurement

EDANS to DABCYL Plus tagged M2 monomers were prepared in ratios of 4:1, 2:1, 1:1, 1:2, 1:4, and 1:8. Fluorescence was measured by a HORIBA Dual Fluorimeter or a Biotek Synergy HT reader. The Dual Fluorimeter was set to 336 nm for maximum EDANS excitation, but an HT Plate reader was used for more reliable measurements. The excitation filter for the HT Plate Reader was 360 nm with a band width of 40 nm and the emission filter was 460 nm with a band width of 40 nm. Delay before sampling was 350 millisecond and delay between samples was 1 millisecond for both. Samples were placed in a 96 sample plate and each buffer pH was repeated in four different wells. Each pH sample was measured four times and averaged.

Results and Discussion

Absorbance of Dye with Change in pH

FRET efficiency should fluctuate with only conformational changes, therefore, both the EDANS and DABCYL Plus dye molecules are required to be pH independent in the experimental pH range. If fluorescence intensity, or absorbance, of fluorophores isolated in solution differ with changing pH, then FRET efficiency with regards to conformational change would be inaccurate. As a result, both fluorophores were tested in order to minimize error from pH associated protonation. Absorbance of free EDANS and DABCYL Plus was measured in varying citrate buffers, ranging between pH 5 and 9.2.

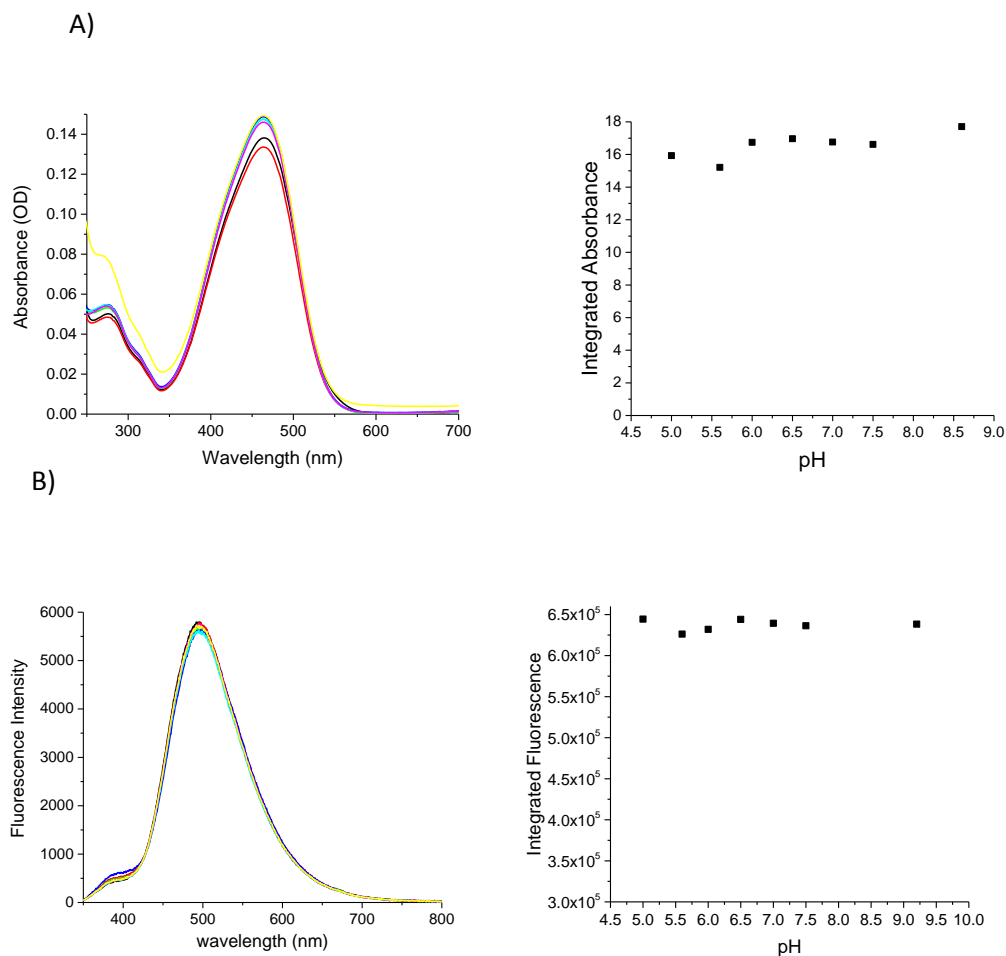


Figure 9. EDANS fluorescence and DABCYL Plus in varying pH.

A) DABCYL Plus absorbance was measured as the DABCYL Plus was added to separate citrate phosphate buffers of pH 5, 5.5, 6, 6.5, 7, 7.5, and 9.2.

B) EDANS fluorescence was found in the same way.

As expected, pH change had no effect on either EDANS or DABCYL Plus absorbance (Figure 9). Therefore, FRET efficiency should only change with M2 dilation response and not pH effect on the fluorophore.

Tetramerization and pH Dependence of M2 Proton Channel

With the addition of fluorophore molecules, the M2 tetramer may not fold properly in the membrane. Adding an extra cysteine residue along with a maleimide fluorophore may

interfere with amino acid residue interactions and tetramer formation. Therefore, a preliminary study was completed to ensure tetramer formation.

With decreasing pH, the four histidine residues become protonated and would repel each other further, increasing the C-termini dilation length. Increased length between the fluorophores should be represented by an increase in EDANS fluorescence intensity, as DABCYL Plus acts as a quencher of EDANS fluorescence. The further EDANS is from this DABCYL Plus quencher, the greater its own fluorescence intensity.

To ensure M2 proton channel tetramerization, amantadine and detergent were added. Amantadine, if tetramers are formed, constricts pore size and reduces C-termini length. Without tetramerization, there are no pores on which amantadine may have an effect. Detergent was added to control samples to promote re-monomerization. If an M2 tetramer has formed, then fluorescence should decrease due to binding of amantadine, as amantadine will decrease C-termini distance. In contrast, when detergent is added, fluorescence should increase as tetramers dissociate without a bicelle environment, and the fluorophore acceptor is no longer in range to quench donor fluorescence. This experiment was conducted at pH 6.51 (Figure 10).

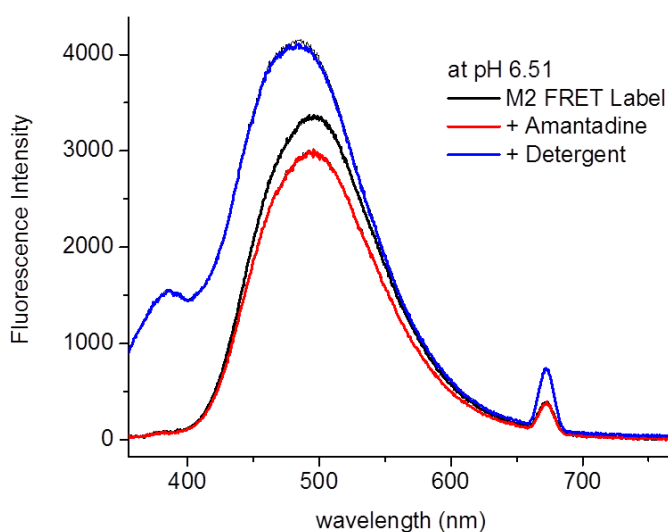


Figure 10. Fluorescence change as amantadine and detergent Tween 20 are added to M2 reconstituted in bicelle DPPC/DHPC. When amantadine was added, the fluorescence dropped. On the other hand, when the detergent was added the fluorescence increased.

As expected, amantadine decreased EDANS fluorescence while detergent increased it. This experiment was repeated in buffer solutions of various pH (Figure 11). EDANS fluorescence intensity decreased with increasing pH. For the first time, the M2 proton channel's conformational change was directly observed in physiologically relevant conditions. C-termini dilation occurred between pH 4.5 and 6. This appeared to be consistent with presumed biologic activity, as the endosome pH is thought to be between 5-6.²

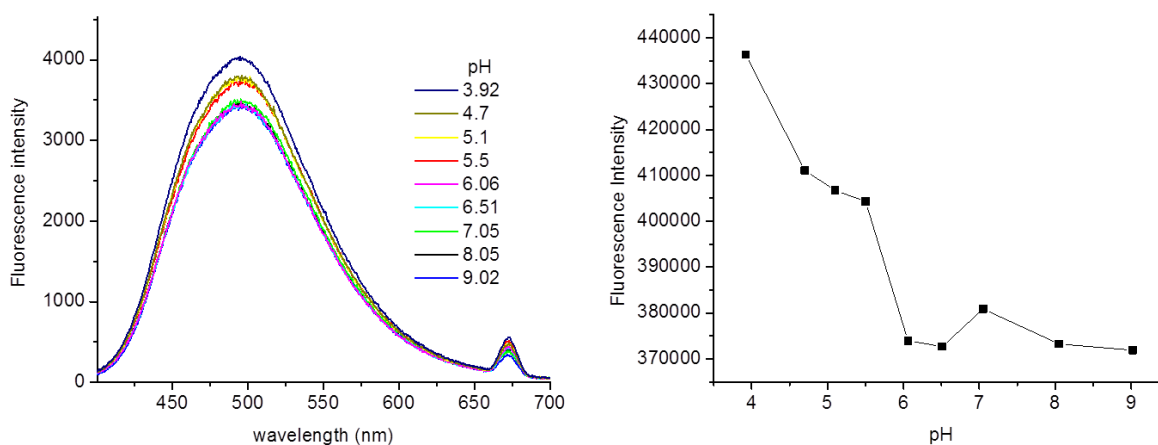


Figure 11. Fluorescence change as the acidity of the M2 tetramers were reconstituted in bicelle DPPC/DHPC. As the acidity increases, the fluorescence increases as well.

The results (Figure 11) indicate to a formation of M2 tetramer and the dilation of the C-termini with increasing acidity.

An additional experiment was completed to consider another interpretation of the results: that the change in EDANS fluorescence may be due to a gradual increase in monomerization at low pH.

M2 monomers, however few that exist, are in constant equilibrium with their tetramer counterparts. As pH decreases, histidine residues protonate and repel each other. This separation may go beyond C-termini dilation to a point of actual tetramer dissociation, thereby increasing EDANS fluorescence, as these preliminary results indicated.

Control experiment: N-termini labeled M2

According to available NMR and X-ray crystal structures, with decreasing pH, N-termini appear relatively rigid, while C-termini are mobile, flexible, and can dilate. In addition, lengths between N-termini are much shorter than lengths between C-termini. Therefore, if tetramerization equilibrium is not a factor, N-termini tagged M2 EDANS intensity should remain relatively unchanged, and much lower than C-termini intensity. If tetramer dissociation is a factor, then N-termini and C-termini fluorescence should be fairly similar in pattern.

To ensure change in EDANS fluorescence is the result of C-termini dilation as opposed to a change in tetramerization equilibrium, a control experiment was conducted. Fluorophores were added to the N-termini of peptides rather than the C-termini. Both C-termini and N-termini fluorescence were measured in the same conditions (Figure 12).

N-termini EDANS fluorescence failed to change with increasing acidity, while C-termini fluorescence increased when exposed to pH decrease from 6 to 4.5 (Figure 12). In addition, N-termini had lower fluorescence intensity than C-termini. The data supports active dilation as opposed to tetramer dissociation.

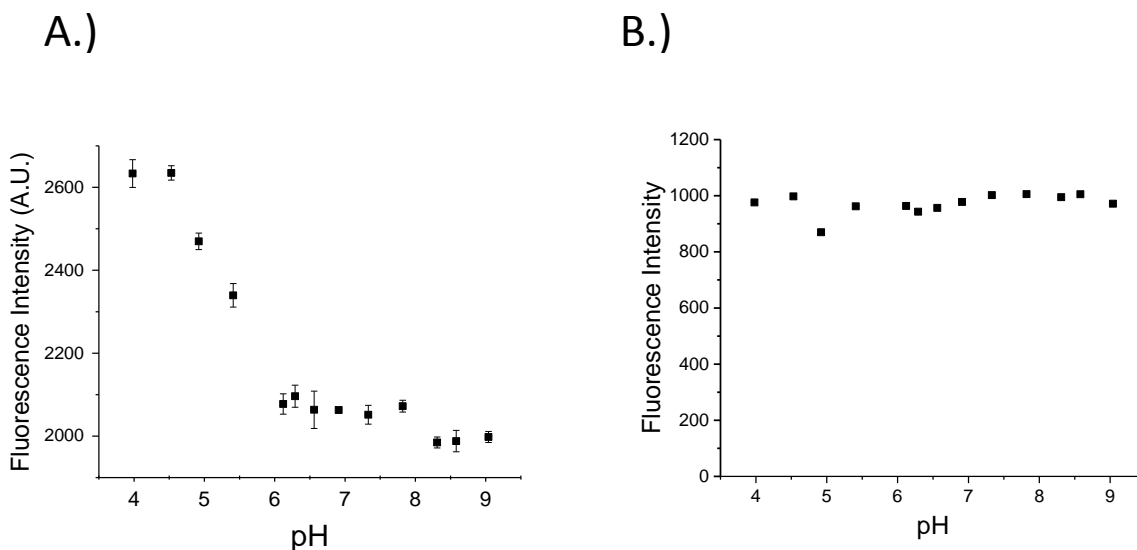


Figure 12. N-termini FRET Experiment

- A) 1:1 DABYCL Plus to EDANS C-termini dyed peptide. Fluorescence intensity of EDANS decreases as pH increases.
- B) 1:1 DABYCL Plus to EDANS N-termini dyed peptide. EDANS fluorescence is unchanged with change of pH.

FRET Efficiency and Distance

To determine the length of the C-termini dilation, FRET efficiency was calculated. There are five possible combinations of donor and acceptor pairs that contribute to the total FRET efficiency of a system (Figure 6). Because of the varying populations of pairs, the three specific identified assumptions must be valid: Random interaction, square configuration, and total tetramerization. This complicates measuring FRET efficiency and length of C-termini dilation. By these assumptions, a FRET efficiency equation was derived for each possible combination of donor and acceptor fluorophore on the M2 proton channel (Table 2). Different ratios of donor and acceptor tagged monomers, given by ratios, 1:8, 1:4, 1:2, 1:1, 2:1, and 4:1. This ratio, termed (r), is the concentration of donor tagged peptide/ concentration of acceptor tagged peptide (D/A). Ratios of selected donor and acceptor tagged peptides are one method to manipulate the

likelihood of possible outcomes of donor-acceptor M2 combinations (Figure 6)⁷. As populations of M2 tetramers change with (r), the overall FRET efficiency will change after correcting for concentration of donor fluorophores (Table 3).

Table 2. The FRET efficiencies of the possible pathways between donor and acceptor pairs.

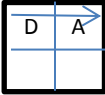
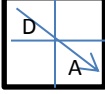
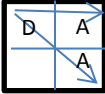
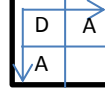
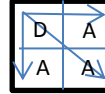
Possible Pathways	FRET Efficiency
 <div style="display: inline-block; vertical-align: middle; margin-left: 20px;">R</div>	$E = \frac{1}{\left(1 + \left(\frac{R}{R_0}\right)^6\right)}$
 <div style="display: inline-block; vertical-align: middle; margin-left: 20px;">$\sqrt{2}R$</div>	$E1 = \frac{E}{(8 - 7E)}$
	$E2 = \frac{E + E1 - 2EE1}{1 - EE1}$
	$E3 = \frac{2E}{1 + E}$
	$E4 = \frac{2E + E1 - 3EE1}{1 + E - 2EE1}$

Table 3. The probability and FRET efficiency of each tagged M2 species in terms of (r) ratio.

Labeling Patterns	Donor/ Acceptor interactions	Channels (Probability) $P_{D_n A_{n-4}}$	No. of Donors	FRET Efficiency $E_{D_n A_{4-n}}^D$				
<table border="1" style="display: inline-table; vertical-align: middle;"><tr><td>D</td><td>D</td></tr><tr><td>D</td><td>D</td></tr></table>	D	D	D	D	N/A	$P = \frac{r^4}{(1+r^4)}$	4	0
D	D							
D	D							
<table border="1" style="display: inline-table; vertical-align: middle;"><tr><td>D</td><td>D</td></tr><tr><td>D</td><td>A</td></tr></table>	D	D	D	A	(Diagonal) (Adjacent)	$P = \frac{4r^3}{(1+r^4)}$	3	$\frac{2E + E_1}{3}$
D	D							
D	A							
<table border="1" style="display: inline-table; vertical-align: middle;"><tr><td>D</td><td>D</td></tr><tr><td>A</td><td>A</td></tr></table>	D	D	A	A	(Diagonal + Adjacent)	$P = \frac{3r^2}{(1+r^4)}$	2	E_2
D	D							
A	A							
<table border="1" style="display: inline-table; vertical-align: middle;"><tr><td>D</td><td>A</td></tr><tr><td>A</td><td>D</td></tr></table>	D	A	A	D	(Adjacent +Adjacent)	$P = \frac{3r^2}{(1+r^4)}$	2	E_3
D	A							
A	D							
<table border="1" style="display: inline-table; vertical-align: middle;"><tr><td>A</td><td>A</td></tr><tr><td>A</td><td>D</td></tr></table>	A	A	A	D	(Diagonal + Adjacent + Adjacent)	$P = \frac{4r}{(1+r^4)}$	1	E_4
A	A							
A	D							

Fluorescence intensities from samples with various donor/acceptor ratios were corrected for concentration. The ratios' fluorescence intensities thereby differ by M2 tetramer donor/acceptor combinations alone. From the corrected fluorescence intensities, FRET efficiency was calculated for each different (r) in varying acidities (Figure 13).

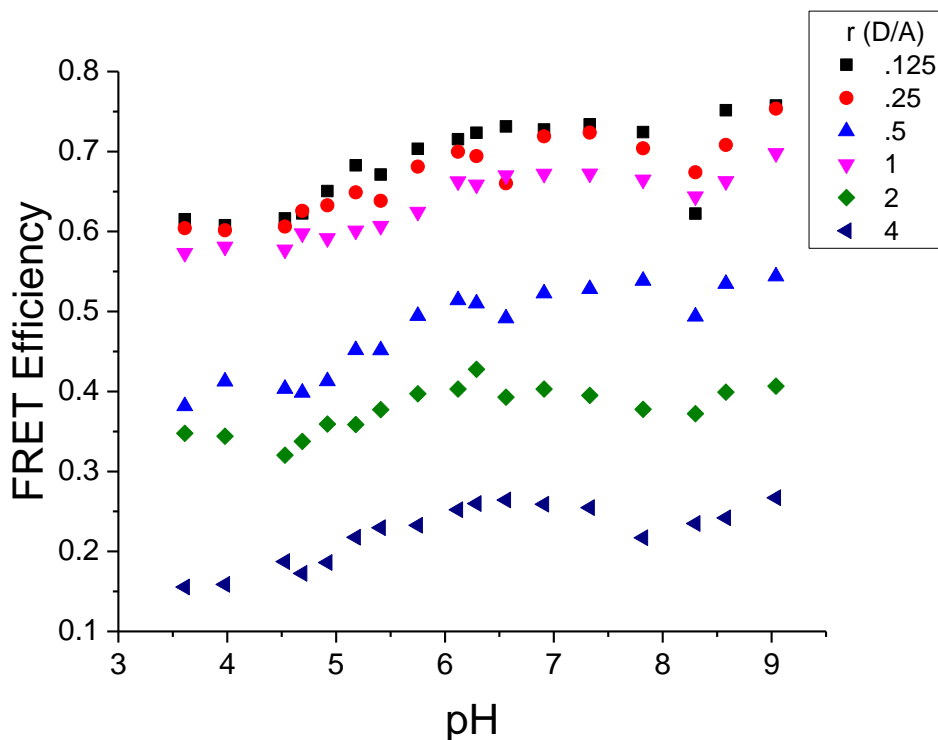


Figure 13. FRET efficiency of M2 responding to pH. Varying (r) ratios change the population of each donor/ acceptor species and therefore change the FRET efficiency corrected for concentration.

The probabilities were calculated for each combination in terms of (r). This probability was multiplied by the number of donors per M2 species and multiplied again by the individual M2 species' FRET efficiency (Table 3).

Total FRET efficiency is a weighted average of the individual M2 tetramer donor/acceptor combinations, represented by the equation:

$$1\text{-FI total} = \frac{\sum_{n=0}^4 n P_{D_n A_{n-4}} (1 - E_{D_n A_n}^D)}{\sum_{n=0}^4 (4-n) P_{D_n A_{n-4}} (1 + E_{D_n A_n}^A \frac{\epsilon_D}{\epsilon_A})}$$

A theoretical FRET efficiency curve, based on the (r) ratio, was calculated and overlaid on experimental data at pH 7.33. Also included is the theoretic population probability of donor/acceptor tetramer for each (r) (Figure 14).

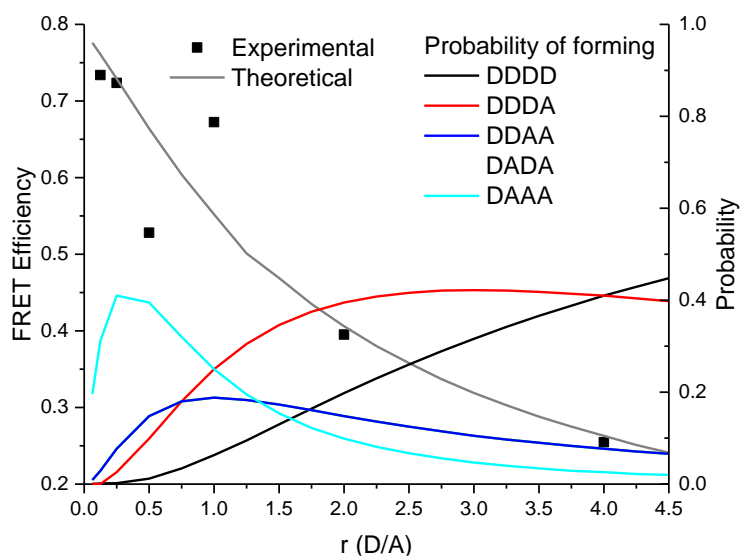
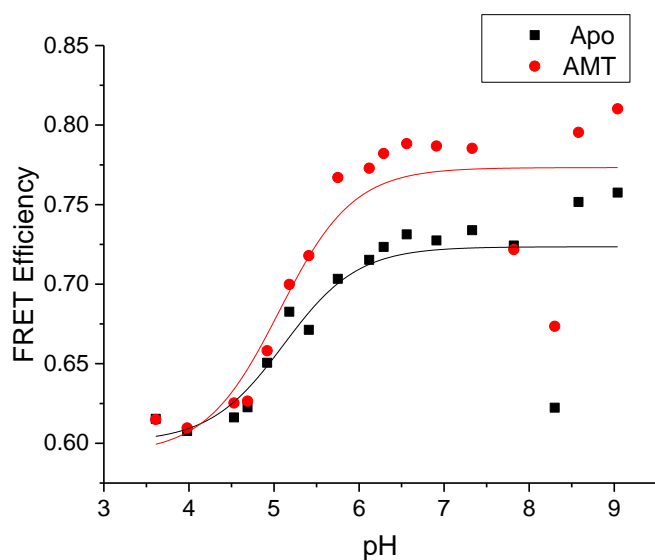


Figure 14. Different D/A ratios at pH 7.33. The Experimental data is overlaid on the theoretical results. Probability of each tetramer species forming also is shown

As predicted, higher (r)'s had lower FRET efficiencies because the combinations that have higher FRET efficiencies were more prevalent. The only outliers were the trials with (r) of .5 and 1. This is likely due to experimental error (Figure 14). There was a clear trend between the experimental and theoretical data. As the frequency of different M2 populations changed, so did FRET efficiency. This supports the presence of a formed tetramer, as the five different M2 species are varying with the (r) ratio.

In addition, the pH and FRET efficiency relationship at (r) =2 and (r) =0.125 was examined in both the drug bound (AMT) and non-drug-bound (APO) forms of the M2 proton channel tetramer.

A)



B)

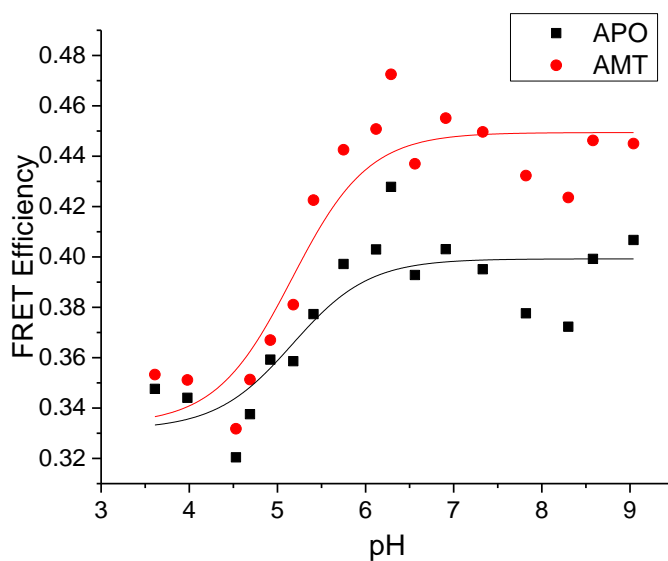


Figure 15. A) pH vs. FRET efficiency curve of (r) =0.125, fit to Henderson-Hasselbalch curve. pKa of 5.1 ± 0.34 while the drug bound state had a pKa of 5.1 ± 0.2 . B) pH vs. FRET efficiency curve of $r=2$. Fitted to Henderson-Hasselbalch curve. pKa of 5.2 ± 0.3 while its drug bound state had a pKa of 5.2 ± 0.2 .

To calculate pK_a, these two graphs were fitted to the Henderson-Hasselbalch equation.

The Apo, (r) =0.125 sample had a pKa of 5.1 ± 0.2 while the drug bound state had a pKa of

5.1 ± 0.3 . The Apo of the $r= 2$ sample had a pKa of 5.2 ± 0.3 while its drug bound state had a pKa

of 5.2 ± 0.2 (Figure 15). Based on pK_a determinations, a correlation is seen between histidine protonation and C-termini dilation length.

After converting FRET efficiency to a distance, the distances for each (r) were averaged. All (r)'s but two outliers of 0.5 and 1, were used, as they failed to follow the fluorescence intensity trend, most likely due to experimental error.

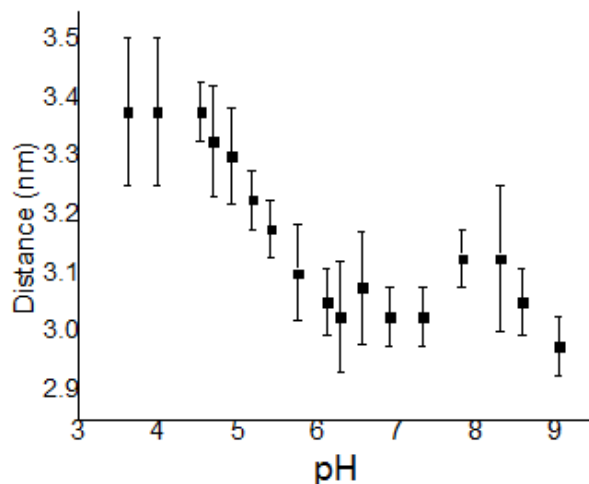


Figure 16. Averaged distance of all the (r) values dependent on pH. Range of 3.0-3.4 nm.

Based on averaged data, the length between two adjacent fluorophores before and after dilation changed from 3.0 to 3.4 nm (Figure 16). A conformational change appears between pH 4.5-6. The adjacent length determined is significantly longer than reported from NMR and X-ray crystal structures, since those lengths are a diagonal distance, not adjacent (Table 2). This discrepancy may be due to the different conditions of X-ray and NMR measurements, such as temperature and crystallization effects. Furthermore, the addition of cysteine, maliemide, and fluorophore molecules required for FRET analysis may also lengthen the average distance. Lastly the influence of the four-fold symmetry assumption changes the results as well.

Discussion

The mechanism of the Influenza A virus M2 proton channel activation is unclear. Clearly, the proton channel is activated in acidic environment such as a late endosome. This step is known to be needed for viral replication. Prior NMR and X-ray crystal structural analyses do not control for all variables necessary to understand the effect of decreasing pH. This paper reports experiments in which monomeric proton channel peptides were synthesized, labeled with donor and acceptor fluorophore, and confirmed to have formed tetramers in bicelle layers. Using FRET analysis in a confirmed biologic acidic environment, the C-termini were shown to dilate with decreases in pH. The length changed from 3.0 to 3.4 nm, with a change in pH from 6 to 4.5. Analysis also showed that FRET changes were truly related to conformational change rather than gradual tetramer dissociation. This conformational change should indicate activation of the M2 proton channel. These novel results were the first to measure the M2 proton channel's conformational changes in a dynamic environment controlling all other factors besides pH.

Improvements to the Experimental Procedure

Lifetime fluorescence measurement is independent of concentration and therefore greater experimental accuracy would be anticipated. EDANS, having a long lifetime of 12 nanoseconds, has a multiple exponential decay and proves quite difficult to measure as a result. Alexa Fluor 546 will therefore be used for future lifetime experiments. Alex Fluor 546 ($\tau = 4.1$ ns) has a single exponential decay and is conveniently also quenched by DABCYL Plus ($R_0 = 2.9$ nm).

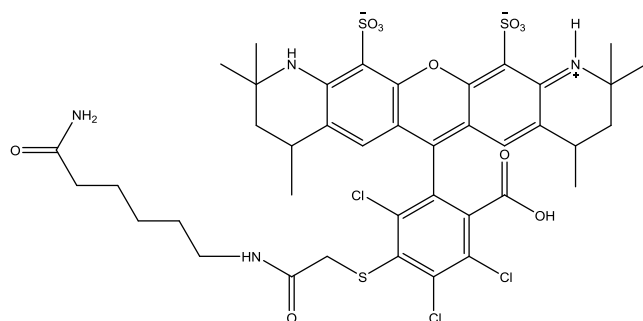


Figure 17. Alexa Fluor 546 chemical structure

Additional experiments would be to ensure that there is in fact proton conduction and if it conformational changes correlate with proton conduction.

References:

- [1] Wiselka M. Influenza: diagnosis, management, and prophylaxis. *BMJ* 1994; 308:1341-1345.
- [2] Pinto, L. H.; Lamb, R. A., Controlling influenza virus replication by inhibiting its proton channel. *Mol Biosyst* 2007, 3 (1), 18-23.
- [3] Acharya, R.; Carnevale, V.; Fiorin, G.; Levine, B. G.; Polishchuk, A. L.; Balannik, V.; Samish, I.; Lamb, R. A.; Pinto, L. H.; DeGrado, W. F.; Klein, M. L., Structure and mechanism of proton transport through the transmembrane tetrameric M2 protein bundle of the influenza A virus. *P Natl Acad Sci USA* 2010, 107 (34), 15075-15080.
- [4] Pielak, R. M., & Chou, J. J. (2011). Influenza M2 proton channels. *Biochimica et Biophysica Acta (BBA)-Biomembranes*, 1808(2), 522-529.
- [5] Lakowicz, Joseph R. *Principles of Fluorescence Spectroscopy*. New York: Springer, 2010. Print.
- [6] Glauner, K. S.; Mannuzzu, L. M.; Gandhi, C. S.; Isacoff, E. Y., Spectroscopic mapping of voltage sensor movement in the Shaker potassium channel. *Nature* 1999, 402 (6763), 813-7.
- [7] Cheng, Wei, Fan Yang, Christina L. Takanishi, and Jie Zheng. "Thermosensitive TRPV channel subunits coassemble into heteromeric channels with intermediate conductance and gating properties." *The Journal of General Physiology* 129, no. 3 (2007): 191-207.
- [8] Glead, M. L., Ioannidis, H., Kolocouris, A., & Busath, D. D. (2015). Resistance-mutation (N31) effects on drug orientation and channel hydration in amantadine-bound influenza A M2. *J. Phys. Chem. B*, 119, 11548-11559.